Accepted Manuscript

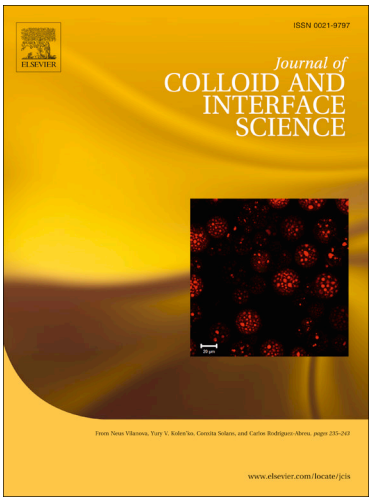

Magnetic Nano-nets for Capture of Microbes in Solution Based on Physical Contact

Venkatesh S. Guruprasad, Vivek Maheshwari

PII: S0021-9797(18)31155-X
DOI: https://doi.org/10.1016/j.jcis.2018.09.079
Reference: YJCIS 24130

To appear in: *Journal of Colloid and Interface Science*

Received Date: 31 July 2018
Revised Date: 17 September 2018
Accepted Date: 23 September 2018

Please cite this article as: V.S. Guruprasad, V. Maheshwari, Magnetic Nano-nets for Capture of Microbes in Solution Based on Physical Contact, *Journal of Colloid and Interface Science* (2018), doi: https://doi.org/10.1016/j.jcis.2018.09.079

Magnetic Nano-nets for Capture of Microbes in Solution Based on Physical Contact

Venkatesh S. Guruprasad[b]*, and Vivek Maheshwari*[a]

a: Corresponding Author, Email-vmaheshw@uwaterloo.ca, Phone: 519-888-4567, ext. 38885, Address- Dept. of Chemistry, Waterloo Institute for Nanotechnology, University of Waterloo, Waterloo ON Canada N2L 3G1

b: Address- Dept. of Chemistry, Waterloo Institute for Nanotechnology, University of Waterloo, Waterloo ON Canada N2L 3G1

ABSTRACT: Self-assembly of Au nanoparticles with Fe ions is used to develop magnetic nano-nets similar to fishing nets for capture and removal of microbes in aqueous medium. The nano-nets have a high aspect ratio, span microns in length with openings of 80-300 nm. This allows them to sample the liquid medium even at low volume fraction and also entrap the microbes in the solution. The nets and the trapped microbes can be effectively pulled from the solution by using an off the shelf magnet. Since the capture is based on physical contact, the nano-nets overcome the ability of the microbes to develop resistance to the cytotoxic effects of chemical compounds and nanomaterials. Using the nano-nets an absolute inactivation of 0.9 is achieved in 5 min. in a non-deaerated solution with Escherichia coli (E. coli). Further the removal of the nano-nets along with the captured microbes also predominantly eliminates the nanomaterial from the aqueous medium for future use.

Keywords- water purification • magnetic chains • nano-nets • gold nanoparticles • self-assembly

1. Introduction

Effective neutralization of microbes in water either by capture or by cytotoxic agents is of critical importance to prevent diseases. This has gained further urgency due to the spread of bacterial resistance to antibiotics[1–4] and increasing scarcity of access to clean water.[5–7] Nanoparticles of Ag, Fe, Au and Fe-oxides are antimicrobial due to generation of oxidative stresses, disruption of cell membranes and cellular processes, and have been extensively researched for this purpose.[8–18] The use of these nanoparticles has also been shown to enhance the effect of antibiotics on bacteria through synergy.[19–21] A rising challenge now is the reported development of microbial resistance to the cytotoxic effects of these nanoparticles.[22] Therefore, nanomaterials that interact and capture the microbes with efficacy by employing alternative strategies are required. To this effect, here we present the use of magnetic nano-nets that are made of Au nanoparticle chains cemented together with Fe-oxides for effective capture of microbes. Unlike 0-Dimensional nanoparticles, these nano-nets have high aspect ratio geometry, which spans microns in size with openings in the range of 80-300 nm. The combined magnetic characteristics of these nets and their ability to sample a greater volume leads to capture of the microbes with great efficacy and also their collection using an off the shelf magnet. Further due to the cytotoxic effects of the constituting materials (Fe oxides) the captured microbes in these nets are also neutralized. These nano-nets effectively combine the physical capture of the microbes due to their geometry with the microbicidal properties of their constituting materials. The removal of these nano-nets from the solution along with the captured microbes also clears the residual water of the nanomaterial which may have adverse effects on its subsequent use.[23,24]

The dimensionality of nanomaterial (and aspect ratio) is a basic physical parameter that critically affects their interaction volume in composites and fluids. For example, the percolation threshold of 1-D materials such as Carbon nanotubes (CNT's) is orders of magnitude smaller than that of spherical nanoparticles.[25,26] The effect of aspect ratio is also seen in thermal conductivity of fluids and composites with nanomaterials as fillers.[27,28] Similar to the effects seen in these processes and parallel to fishing nets used for capture of aquatic organisms, the developed nano-nets function as an effective means for both physical capture and cytotoxic effects induced neutralization of the microbes. The neutralization of microbes using nanomaterials can be considered a two-step process. First there has to be a direct contact (or close proximity) between the microbe and the nanomaterial in the fluid environment. Success in this step is required for both physical capture of the microbe and also to induce cytotoxic effect on the microbe. The second step is the nanomaterials inducing the cytotoxic effects on the microbe as a result of the direct contact or close proximity. The effect of having a net like nanomaterial is two fold; first due to its high aspect ratio even a small volume fraction of the nets is able to sample a large volume in water, similar to the percolation effects in composites.[25,26] This greatly increases the probability of contact between the microbe and the nets, satisfying the first step for capture of the microbe. Second as the material is organised into a large network, the interactions with the microbes are at a greater scale than compared with those of single nanoparticles. We show that using these magnetic nano-nets E. coli in the concentration of $1.6x10^6$ colony forming units (CFU) can be removed from solutions in less than 5 min with more than 90% efficiency. Further the capturing ability of these nano-nets based on their volume fraction in solution and the number density of the target species is characterized using 1 micron Poly(methyl methacrylate) (PMMA) microspheres and also E. coli. By using Au nanoparticles, the minimum size of particles that can be effectively captured by the nano-nets is found to be

100 nm. Also we show their effectiveness in capturing microbes with different physiology by using a mixture of E. coli (a prokaryotic gram negative bacteria) and Saccharomyces Cerevisiae (S. cerevisiae, bakers yeast, a eukaryotic microbe) in water and also towards Bacillus Subtilis (a prokaryotic gram positive bacteria).

2. Experimental

2.1 Materials

E. coli strain ATCC 47046, Saccharomyces cerevisiae (yeast) BY4741 are purchased from ATCC. Bacillus Subtilis (Strain 168) was kindly supplied by Prof. Trevor Charles group at University of Waterloo. Au nanoparticles (10 nm with concentration $5.7x10^{12}$ particles/ml; 50 nm with concentration $4.5x10^{10}$ particles/ml and 100 nm with concentration $5.6x10^{9}$ particles/ml) were purchased from Ted Pella (unconjugated gold colloid manufactured by BBI International). Yeast Extract-Pepton-Dextrose (YPD) broth and Nutrient broth No. 1 were purchased from Sigma-Aldrich. $FeCl_2.4H_2O$ (> 99% purity), $FeCl_3.6H_2O$ (> 99% purity) and $NaBH_4$ (> 98% purity) were also purchased from Sigma-Aldrich and used as such. 1 µm sized PMMA microspheres were purchased from Sigma-Aldrich (10% by volume). All the glass vials, caps, pipette tips and Millipore water were autoclaved to sterilize the equipment for elimination of any possible contaminants.

2.2 Material Characterization

Ultraviolet-visible (UV-Vis) spectroscopy was carried out by using MINI-D2T deuterium tungsten light source and USB4000 Miniature fiber optic spectrometer from Ocean Optics. Field emission scanning electron microscopy (FESEM) was used to evaluate morphologies of the samples and study them. Images were taken by using ULTRA PLUS and Leo 1530 from Carl Zeiss. Transmission electron microscopy (TEM) images were obtained with a LEO 912ab

transmission electron microscope. X-ray diffraction (XRD) patterns were obtained from the samples deposited on a silicon substrate with a native oxide layer using a glancing incidence X-ray diffraction (GIXRD) using a PANalytical X'Pert Pro MRD diffractometer with Cu Kα radiation (λ= 1.54 Å) at an incidence angle of 0.4°. X-ray photoelectron spectroscopy (XPS) was used to study the oxidation state and compositions of the iron oxide-gold nanoparticle composite. The instrument used for this purpose was Thermo-VG Scientific ESCALab 250 Microprobe equipped with a monochromatic Al K-alpha X-ray source (1486.6 eV). Zeta Sizer Nano ZS90 from Malvern Instruments was used for measuring both zeta potential and size distribution of our samples. Optical microscope DMI 3000 B from Leica equipped with a Hamamatsu CCD was used for optical imaging.

2.3 Assembly and Formation of Nano-nets

270 μL of a solution containing both 1 mg/mL $FeCl_2$ and 2.718 mg/mL $FeCl_3$ dissolved in Millipore water was added to a glass vial which contains 4.0 mL of the stock Au nanoparticles. The final solution was put on a shaker for eight hours for assembling of Au nanoparticles. As the 10 nm Au nanoparticles interact with the Fe^{2+} and Fe^{3+} ions and self-assemble into chains, the solution mixture becomes blue in color. 600 μL of 10 mg/mL $NaBH_4$ was added to the Au-Fe nanoparticle chains to reduce Fe^{2+} and Fe^{3+} ions to Fe^0. The Fe on contact with air is oxidized immediately (within 15 – 30 minutes) to Fe_2O_3. The composite in the vial is now magnetic and the gold chains can now be pulled with the help of a handheld magnet. Magnets are ¾ inch ceramic disks sold by Hillman. 4-8 pieces of magnet stacked on top of each other are used to pull the chains on to the sides of the vial which can be easily removed later.

2.4 Bacterial Concentration Determination

Nutrient agar plates were prepared by dissolving 2.8g of nutrient agar in 1 litre of water and autoclaving the solution at 121° C for fifteen minutes. The solution was cooled until it reached 40°-50° C and then poured into petri-dishes. CFUs were determined by plating the solution before and after extraction of the bacteria (or as required) on the Agar plates and after being incubated overnight at bacteria growing conditions (37° C and no light exposure). The CFU was calculated using the formula: CFU/ml = (no. of colonies x dilution factor) / volume of culture on plate. The microspheres and the microbes were also counted using Brightline haemocytometer made by Hausser Scientific and following the accompanying instructions.

3. Results and Discussion

The nano-nets are made by mixing Au nanoparticles (10-12 nm in diameter, $5.7x10^{12}$ particles/ml) with Fe^{3+}/Fe^{2+} ions in a pre-determined optimal concentration (0.34 mM of Fe^{2+} and 0.68 mM of Fe^{3+}, details in experimental section). These Au nanoparticles have a zeta potential of ~ -33 mV due to the presence of citrate molecules on their surface. [29] As a result of the interaction between the multivalent cations Fe^{3+} (and Fe^{2+}) and their surface anionic groups the nanoparticles assemble into microns long branched chain like structures.[30–34] A typical morphology of these chains can be seen in the TEM image of Figure 1a. The higher magnification image of Fig. 1b (and its inset) shows that openings of size 80-300 nm are observed between these chains. Also there is ~ 1-2 nm spacing between the adjacent nanoparticles due to the Fe ions. The Fe ions are then reacted to form Fe-oxides (details in experimental section), which transforms these chains into continuous structures similar to nano-nets. The TEM images of Fig. 1c (and inset) show that the chains are continuous in nature following the transformation. The concentration of cations (Fe^{2+} and Fe^{3+}) in the Au nanoparticle solution is critical for the assembly process. Au nanoparticles in absence of any cations (Fe^{2+} and

Fe^{3+}) are isolated from each other due to negative zeta potential, as seen in the TEM image of Fig. 1d. If the concentration of the cations (Fe^{2+} and Fe^{3+}) is reduced to half (of the optimal concentration) the scale of the assembly is significantly reduced (TEM image of Fig. 1e). Similarly, if the concentration of the cations is doubled the Au nanoparticles agglomerate due to the high ionic strength of the solution as seen in TEM image of Fig. 1f.

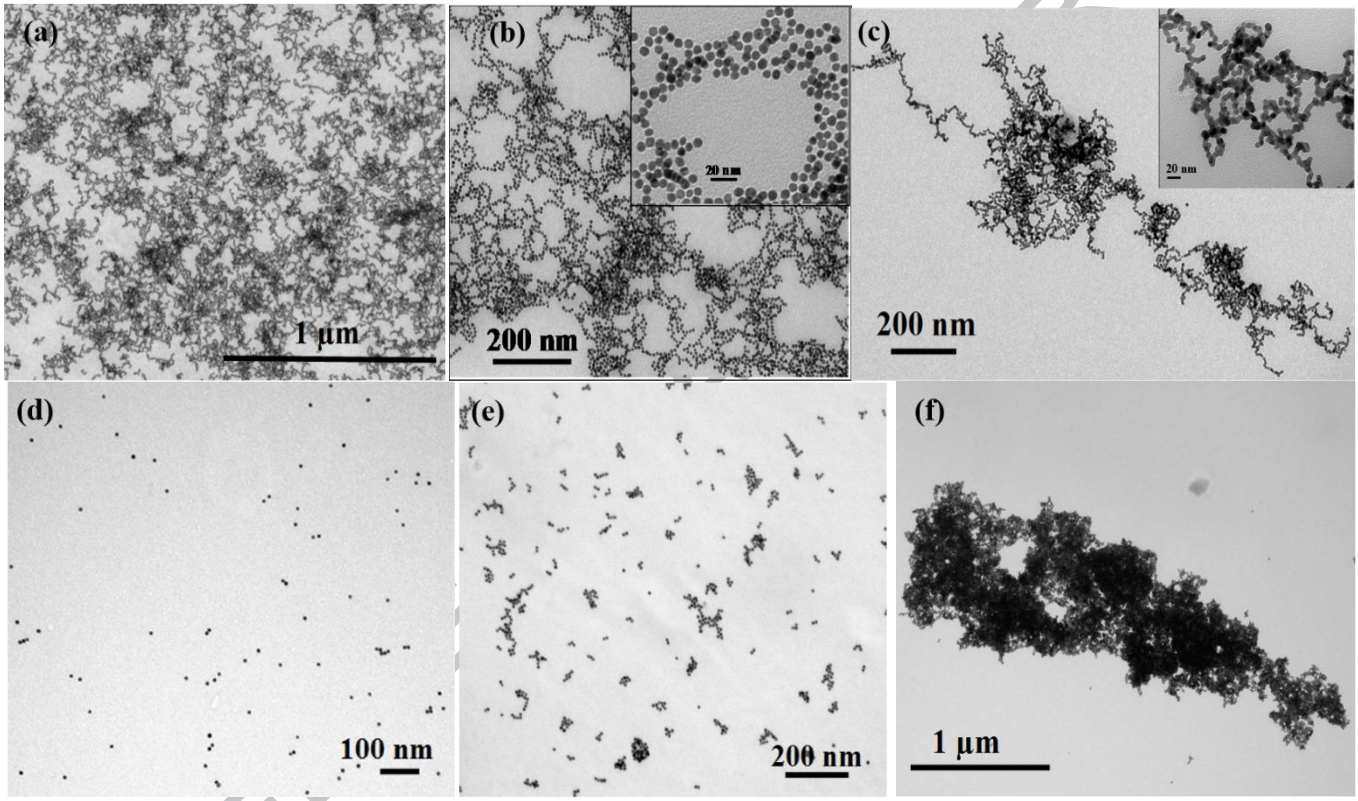

Figure 1. TEM images of the assembly of Au nanoparticles by use of Fe ions and their subsequent transformation to magnetic Au-Fe oxide nano-nets. (a) Au nanoparticles chain like assembly with use of Fe ions in optimal concentration. (b) Higher magnification images of the chains. Scale bar in the inset is 20 nm. (c) Images following the transformation of the Fe ions to Fe oxide. (d) Image of plain Au nanoparticles in absence of added Fe ions. (e) Image of the Au nanoparticles on adding half of the optimal amount of Fe ions required for assembly (f) Image of Au nanoparticles on doubling the concentration of the Fe ions.

The formation of the Fe oxides in the Au chains is confirmed by a variety of characterization techniques. X-ray diffraction result of Fig. 2a shows the peaks corresponding to

Au and weak ones corresponding to Fe_2O_3.[35,36] The presence of Fe_3O_4 cannot be ruled out due to close proximity of the peaks between these two Fe-oxides, supporting the conclusion that these are mixed oxides in nature. The XPS results also show the formation of the Fe-oxides (Fig. 2b, survey spectra; Fig. 2c Fe 2p; Fig. 2d, O 1s). The Fe $2p_{3/2}$ and Fe $2p_{1/2}$ peaks are centred at the binding energies of 711.3 eV and 724.8 eV which are the typical values for Fe^{3+} in Fe_2O_3.[37,38] A satellite peak of the main Fe $2p_{3/2}$ which is located centred at 719.4 eV further indicates the presence of Fe^{3+} species.[38] The O peak centred at 530.2 eV pertains to the lattice oxygen of Fe_2O_3, while the O peak located at 532.5 eV corresponds to the oxygen defects in the metal oxide matrix and the O in SiO_2.[38–40] The O peak at 532.5 eV is higher in intensity than the first because the XPS measurements were performed on Silicon substrates which contributes to a higher intensity signal. These observations support the conclusion that Fe ions in the chains transform to Fe-oxides and are composed of predominately Fe^{3+} oxides. The reaction of the Fe ions into Fe-oxides also makes these chains magnetic. The spectra for Au 4f are presented in the supporting information (SI). The optical images of Fig. 2e show that on applying a magnetic field using an off the shelf magnet, the chains are completely pulled out and the solution loses color. The UV-Vis absorption spectra presented in Fig. 2f further show these transformations. The plain Au nanoparticles have a typical surface plasmon resonance (SPR) peak at ~ 525 nm, on assembling into branched chains this peak shifts to ~ 627 nm due to the over lap of the SPR between adjacent nanoparticles as their separation is ~ 1-2nm (Fig. 1a&b).[41,42] On reducing the chains to form the nano-nets the spectra shows a broad absorption due to the Fe-oxide nanostructures.[43,44] On pulling out the nets from the solution using a magnet, the UV-Vis shows a flat line attesting to the removal of the Au-Fe nano-nets and their magnetic nature. Both

the reduced and unreduced chains have a zeta potential of ~ -30 to -40 mV leading to their stability in water (see SI for details).

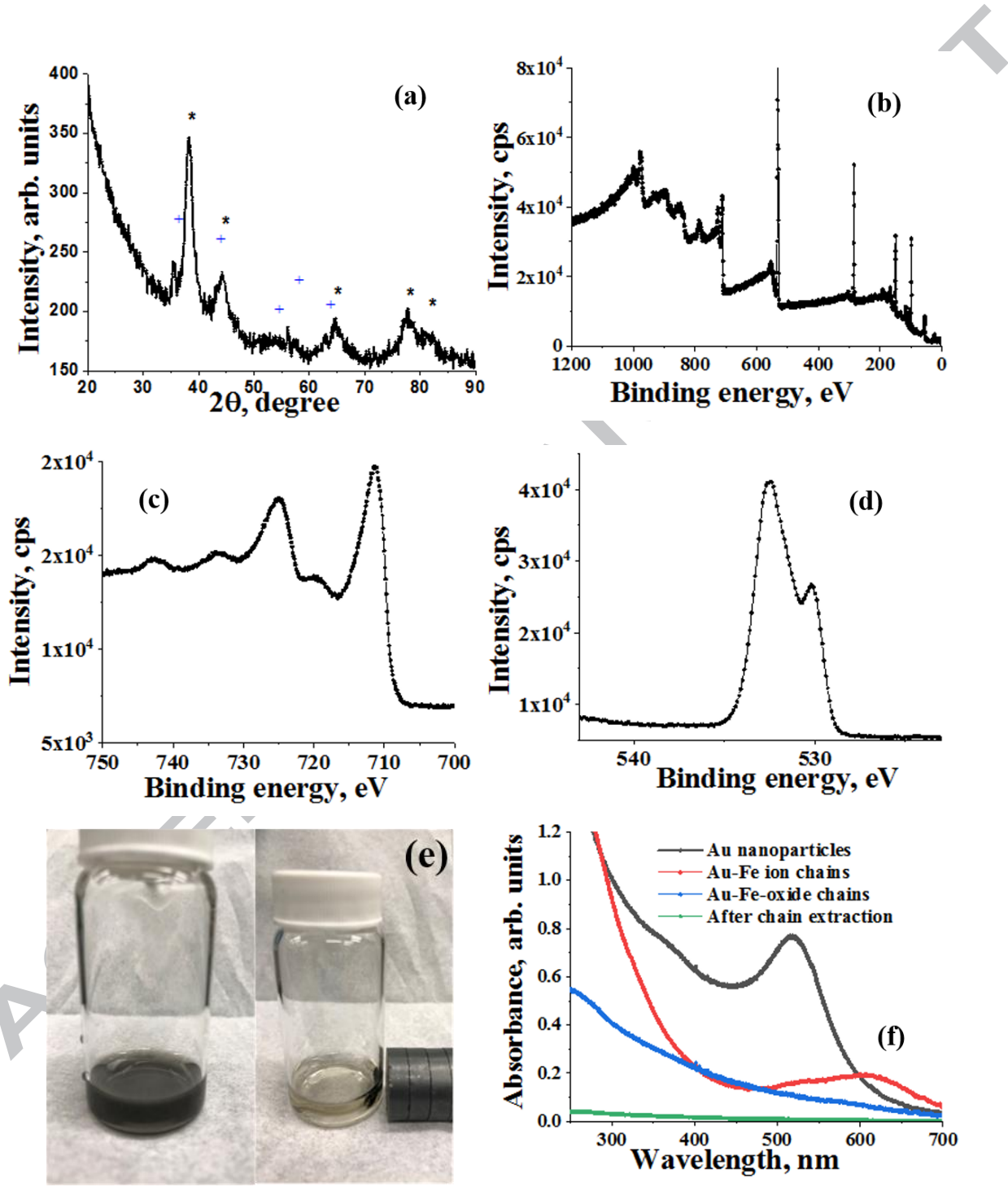

Figure 2: Characterization results for the magnetic Au-Fe-oxides nano-nets. (a) The XRD spectrum shows peaks corresponding to Au (*) and Fe_2O_3 (+). (b) The survey spectrum from

XPS. (c) The Fe 2p spectrum (d) The O 1s spectrum. (e) The optical image on the left shows the stable colloidal solution of the nano-nets, on right the nano-nets are pulled out of the solution by using an off the shelf magnet. (f) The UV-Vis absorption spectra of, colloidal Au nanoparticle solution (grey), their chain like assemblies by use of Fe ions (red), nano-nets on formation of Fe oxides (blue) and following their extraction of the residual solution (green).

The ability of these nano-nets to extract microbes from water is shown by adding them to a solution of the E. coil cells. The microbes are present in concentration of $2.0x10^6$ CFU/ml, and the concentration of Fe added is 0.053 mg/ml (0.95mM). After the addition, a magnet is used to swirl the nano-nets in the solution for 1 min and then held stationary to pull them out. Subsequently using Agar plates (images in SI) the viable microbe concentration in the solution after extraction is determined to be $2.5\ x10^5$ CFU/ml (the average of three replicates). This provides an inactivation ($\log(N/N_0)$; N is the remaining and N_0 is the initial CFU/ml) of -0.9 for the nano-nets. The nano-nets effectively remove more than 87% of the microbes in less than 5 min. This leads to E. coli inactivation efficiency of 0.2 log(inactivation)/(mg/L . h). The removal of the E. coli from the solution is also confirmed by counting the cells using a hemocytometer which provides an E. coli concentration of 2.9×10^5 cells/ml in the residual solution (the average of three replicates). These results show that the nano-nets are effective in physically capturing and removing the E. coli from the solution. The concentration of Fe used here is comparable to that of plain Fe[11,16] and Ag[8,9] nanoparticles used as anti-microbial agents. Further this is achieved in a non deaerated solution within 5 minutes, simplifying the use of nano nets, unlike deaerated solution[11] typically used for achieving high efficiencies with Fe based nanoparticles. The removed nano-nets show a high density of the E. coli cells attached to them as observed in the FESEM images of Figure 3a&b. The TEM images of Fig. 3c&d show that the Au-Fe nano-nets attach to the surface of the microbes at multiple places (circled in red in Fig. 3d and its inset). This multi point interaction over a large area of the microbes allows them to be pulled

with the nano-nets on applying a magnetic field. The microbes appear dark in TEM images due to the attachment of these nets which are made of transition metals (Fig. 3c&d). In contrast a plain microbe appears semi-transparent (inset of Fig. 3c). On plating these nano-nets with the extracted microbes on Agar plates (images in SI) the viable CFU were reduced by 80%. This shows that the cytotoxic effect of the Fe oxides in the nano-nets neutralizes the extracted microbes. The magnetic nano-nets hence have a dual action, first due to their high aspect ratio and net like structure they are able to physically capture the microbes with high efficacy from the solution (as seen from the agar plating, hemocytometer counting, and electron microscopy images) and hence act as effective microbial extraction agents. Second, as an added benefit following the extraction due to the close proximity between the microbes and Fe-oxides in the nano-nets their cytotoxic effect leads to neutralization of the captured microbes (as seen from the agar plating results). The reusability of the nano-nets following one extraction is gauged by again using them in a second identical cycle of microbe capture. In this case using the cell counter and counting of the CFU units an extraction efficiency of 60 % is determined in the second cycle. The nano-nets hence can be effectively applied for at least two cycles.

A mixture of E. coli (a gram negative prokaryotic microbe) and S. cerevisiae (a eukaryotic microbe) is also subject to successful removal by the Au-Fe nano-nets, as can be seen in the FESEM images of Fig. 3e&f, where both these microbes can be clearly seen attached to the nano-nets. The nano-nets capture both the microbes with similar effectiveness as determined by their initial ratio in the solution and that in the extracted nano-nets. Both these microbes have a negative zeta potential[45] (see SI) and hence their interaction with the nets is not based on electrostatic interaction. The ability of the nano-nets to capture a variety of microbes is further confirmed by using them to successfully capture gram positive bacteria Bacillus Subtilis, as seen

in the FESEM images of Fig. 3g&h. The nano-nets can be clearly seen attached to the microbes. Hence the nano-nets can successfully target a variety of microbes and can be used as a generic method for their extraction.

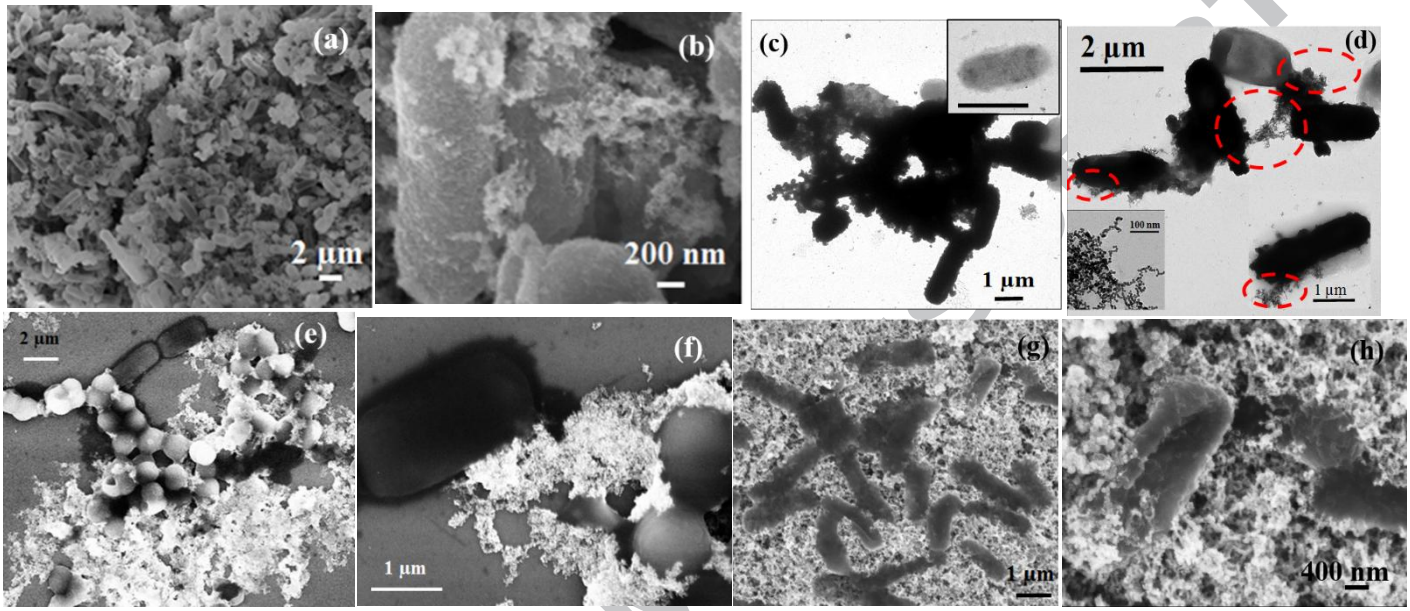

Figure 3. The use of the magnetic nano nets to successfully pull out E. Coli, S. cerevisiae and Bacillus Subtilis from water. (a) The FESEM image of the pulled out nano nets from a E. coli contaminated water. (b) A higher resolution FESEM image of the pulled out nano-nets. (c) TEM image of the pulled out nano-nets and the E. coli. The inset is a plain E. coli cell. Scale bar in the inset is 2 µm (d) High magnification TEM of the nano-nets and the captured E. coli cells. Scale bar in the left inset is 100 nm. (e) FESEM image of nano-nets pulled from a solution of E. coli and S. cerevisiae (f) High magnification FESEM image of the nano-nets are attached to both the microorganisms. (g) FESEM image of the nano-nets and the captured gram positive bacteria Bacillus Subtilis (h) A high magnification image shows the nano-nets attached to the surface of Bacillus Subtilis.

Two set of control experiments are conducted to evaluate the effect of just the Au nanoparticles on the E. coli microbes (each experiment is conducted in triplicate for error analysis). For the first experiment, three identical sets of E. coli contaminated solutions each with a 2.0×10^6 CFU/ml are prepared. Then to the first solution just plain Au nanoparticles, to the second solution the nano-nets, and in third solution just plain autoclaved water is added (as control). Both the first and second solution have identical Au nanoparticle concentration of 4.56 x 10^{12} particles/ml. The second solution due to the presence of Fe-oxides in the nano-nets also

has Fe concentration of 0.95 mM. Following 5-10 min incubation, the nano-nets are extracted from the second solution. The four samples are then plated on Agar for determining the CFUs (images in SI). The results are shown in Fig. 4a. The solution with just E. coli and water (control) shows a microbial concentration of 2.1 x 10^6 CFU/ml, the solution with only Au nanoparticles shows a slight reduced microbial concentration of 1.8 x 10^6 CFU/ml. In contrast the extracted nano-nets have a microbial concentration of 4.1 x 10^5 CFU/ml and the solution left following the extraction of the nano-nets has 2.52 x 10^5 CFU/ml. These results show that the Au particles by themselves have limited cytotoxic effects and also cannot be extracted from the solution as they are non-magnetic, while the nano-nets have dual effect, they combine the cytotoxic effects of the Fe-oxides with physical capture of the microbes. To further confirm the limited cytotoxic effect of the Au nanoparticles in contrast to the nano-nets dynamic shake flask method is also used as the second control experiment.[46] The growth curve of Fig. 4b clearly show that the nano-nets due to the presence of Fe oxides have cytotoxic effects on the microbes which significantly reduces their CFU count and leads to a lag in their growth, while the Au nanoparticles have a little or no effect in this regard.

The ability of the nano-nets in terms of the size of contaminants that can be captured is characterized by using 100 nm and 50 nm Au nanoparticles. Both these nanoparticles also have a negative zeta potential (see SI for details) and hence do not have electrostatic interaction with the nano-nets which also have a negative zeta potential (see SI). This is unlike the interaction between the oppositely charged Fe^{2+} and Fe^{3+} cations and the negatively charged Au nanoparticles that leads to the formation of the Au-Fe ion chains. First using a solution of 100 nm Au nanoparticles (concentration of 5.6x10^9 particles/ml) is mixed with Au-Fe nets, similar to the microbe extraction, after swirling the nano-nets they are extracted using a magnet. The FESEM images (Figure 4c&d) show that the nets are successful in capturing the 100 nm Au

nanoparticles. This shows that the nano-nets are able to capture 100 nm size particles effectively. Similar process is repeated with 50 nm Au nanoparticles and following the extraction of the nano-nets their FESEM image (Fig. 4e) shows that hardly any of the nanoparticles are captured and most of them remain in the solution. The nano-nets hence due to their morphology can effectively extract particles of size larger than 100 nm.

Figure 4. Control experiments showing the effect of Au nanoparticles and the nano-nets on the microbes; The minimum size of the nanoparticles that can be extracted by the nano-nets. (a) The effect on E. coli based on CFU count due to exposure to Au nanoparticles and the nano-nets. (b) Results from the dynamic shake flask method on exposure of the E. coli to Au nanoparticle and the nano-nets. (c) FESEM images of the nano-nets pulled from 100 nm Au nanoparticle solution. (d) Higher magnification images of the extracted nano-nets with attached 100 nm Au

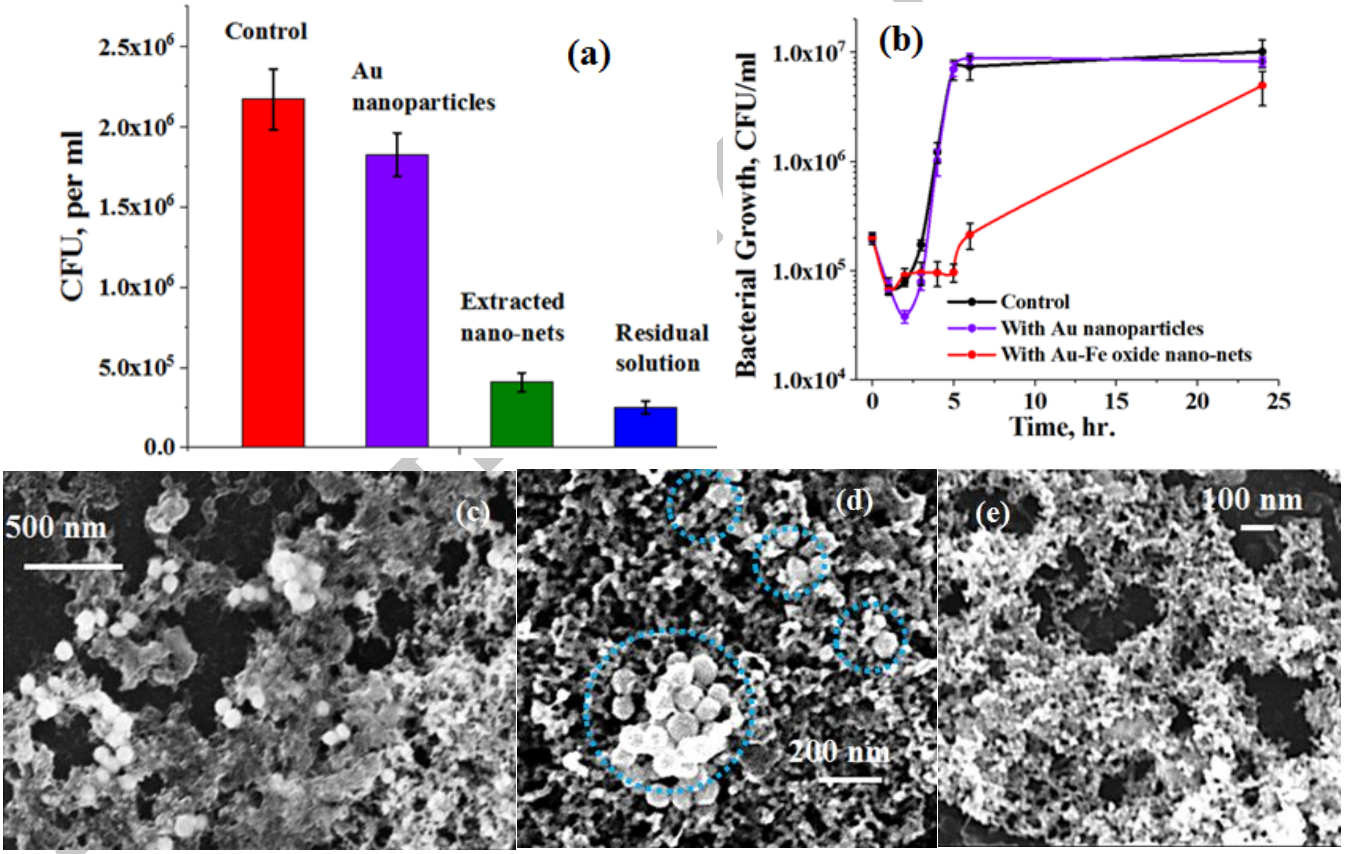

nanoparticles. (e) FESEM image of the extracted nano-nets from 50 nm Au nanoparticle solution.

The interplay between the capture efficiency of the nano-nets based on, their volume fraction in the solution and the concentration of the target species is characterized by a series of experiments. This is done by adding the nano-nets to a solution of PMMA microspheres that

have a size 1 μm and a negative zeta potential (-44 mV, see SI), similar to microbes. The PMMA

microspheres are used due to their well-defined size and number density in solution. First we

conduct the capture of the PMMA microspheres by increasing their concentration in solution

while keeping the number of nano-nets constant. Figure 5a shows that the capture efficiency

follows a S-shaped curve (inverted) on increasing the microsphere concentration. This is related

to the saturation of the collection by the nano-nets as they reach their capacity to interact with the

microspheres. The line is a fit based on power law. A parallel experiment is then performed with

E. coli and as seen in Fig. 5a (blue curve) a result similar in nature to that of the microspheres is

obtained, this attests to the viability of using the microspheres in these experiments. In the

second experiment the concentration of the PMMA microspheres is kept constant at 1.15×10^6 microspheres/ml in the solution and the volume fraction of the nano-nets is varied from ~ 5×10^{-4} to 1×10^{-3} %. The capture efficiency of the nets is shown in Fig. 5b. We observe a typical S-shaped curve with capture efficiency increasing from 1.6% to 90% with increasing nano-net volume fraction. The line curve in the figure is the fit done using a typical power law. This result is similar in nature to the rise in electrical conductivity of a composite with increasing volume fraction of a conductive filler.[47] We observe from both these analyses that 50% capture is achieved at nano-net volume concentration of 7.8×10^{-4}% and at PMMA microsphere concentration of 3.1×10^6 particles/ml. There is however an interplay between the two parameters. The limiting number of particles that can be captured is governed by the maximum capacity of the nano-nets as shown in Fig. 5c. Also the ability to capture the particles is dependent on the volume fraction of the chains that dictates their interaction frequency with the PMMA microspheres, below a critical volume fraction this ability decreases drastically.

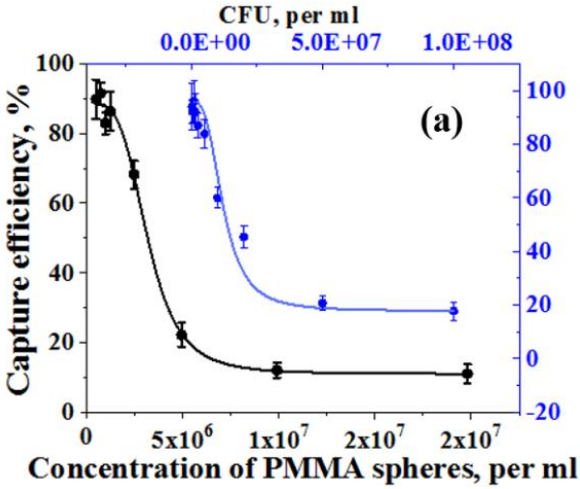

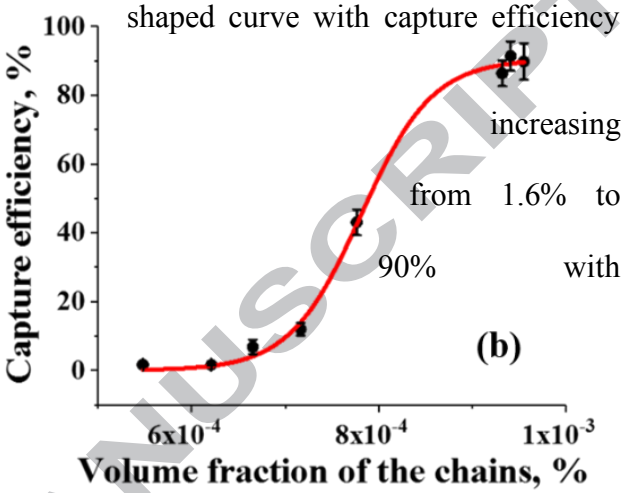

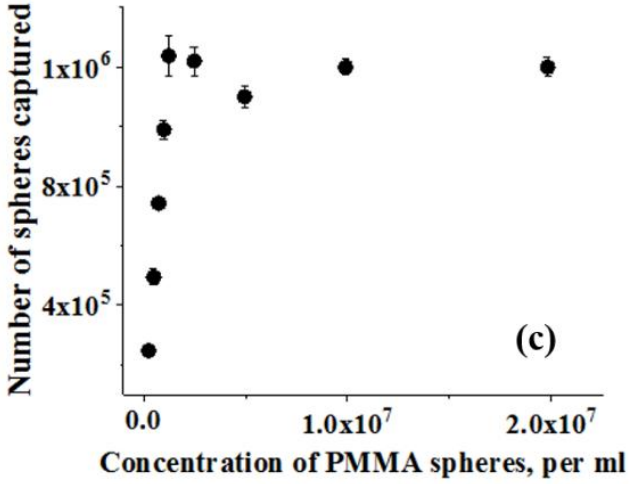

Figure 5. The efficiency of the nano-nets for extracting the PMMA microspheres and the microbes is evaluated and fitted using a power law model. The error bars are based on three sets of replicates for each experiment (a) With a constant nano-net concentration on increasing the microsphere and the microbe concentration both show an inverse S-shaped decay in capture efficiency. (b) For a constant microsphere concentration the extraction efficiency follows an S-shaped curve with the volume fraction of the nano-nets. (c) On increasing the microsphere numbers we observe that the collection by a fixed number of nano-nets reaches a saturation limit.

4. Conclusions

The dimensionality of nanomaterials is an important parameter governing their interaction volume with surrounding medium as has been shown for conductive composites.[26] By applying this principle and similar to fishing nets we have designed magnetic nano-nets made of Au and Fe oxides that combine physical interaction with cytotoxic effects for efficient capture of microbes. As a result, due to their diffuse morphology these nano-nets can be used in very small concentrations for capture and extraction of microbes from solution with high efficacy using an off the shelf magnet. This also serves to clean the residual solution of any nano-nets

used during the process.[48] The minimum size of particles that can be extracted using these nano-nets is ~100 nm, which is limited by the size of their openings as governed by their self-assembly process. The extraction efficiency of the nano-nets depends on their concentration in the solution as it dictates their interaction volume with the fluid. Since the presented approach uses physical capture of the microbes for their extraction, it will be useful in addressing the challenge of developing microbial resistance to the cytotoxic effects of both anti-biotics and nanomaterials. [2-4, 22] Such new strategies are also required due to the increasing range and frequency of water borne tropical diseases related to the changing climate patterns.[49-51] We believe that such strategies based on the ability to make nanomaterials with varying morphology, resulting in physical means to target and neutralize microbes and hence circumventing the need to have a physiological interaction with them, presents a viable option for the future of water purification.

Acknowledgement

The authors acknowledge financial support from Natural Sciences and Engineering Research Council of Canada, Canada Foundation for Innovation, Ministry of Research, Innovation and Science Ontario and University of Waterloo. We also thank Prof. Trevor Charles and Adrian William Van Dyk for providing the Bacillus Subtilis Strain 168 sample.

REFERENCES

[1] A. Martins, G. Spengler, J. Molnár, L. Amaral, Bacterial Antibiotic Resistance, in: eLS, John Wiley & Sons, Ltd, Chichester, UK, 2014: pp. 1–11.

doi:10.1002/9780470015902.a0001993.pub2.

[2] P.S. Stewart, J. William Costerton, Antibiotic resistance of bacteria in biofilms, Lancet. 358 (2001) 135–138. doi:10.1016/S0140-6736(01)05321-1.

[3] S.N. Cohen, A.C.Y. Chang, L. Hsu, Nonchromosomal Antibiotic Resistance in Bacteria: Genetic Transformation of Escherichia coli by R-Factor DNA, Proc. Natl. Acad. Sci. 69 (1972) 2110–2114. doi:10.1073/pnas.69.8.2110.

[4] E. Banin, D. Hughes, O.P. Kuipers, Editorial: Bacterial pathogens, antibiotics and antibiotic resistance, FEMS Microbiol. Rev. 41 (2017) 450–452. doi:10.1093/femsre/fux016.

[5] M. Elimelech, The global challenge for adequate and safe water, J. Water Supply Res. Technol. - Aqua. 55 (2006) 3–10. doi:10.2166/aqua.2005.064.

[6] K. Onda, J. LoBuglio, J. Bartram, Global Access to Safe Water: Accounting for Water Quality and the Resulting Impact on MDG Progress, Int. J. Environ. Res. Public Health. 9 (2012) 880–894. doi:10.3390/ijerph9030880.

[7] S. Damkjaer, R. Taylor, The measurement of water scarcity: Defining a meaningful indicator, Ambio. 46 (2017) 513–531. doi:10.1007/s13280-017-0912-z.

[8] A. Panáček, L. Kvítek, R. Prucek, M. Kolář, R. Večeřová, N. Pizúrová, V.K. Sharma, T. Nevěčná, R. Zbořil, Silver Colloid Nanoparticles: Synthesis, Characterization, and Their Antibacterial Activity, J. Phys. Chem. B. 110 (2006) 16248–16253. doi:10.1021/jp063826h.

[9] C. Chen, C. Chiang, Preparation of cotton fibers with antibacterial silver nanoparticles, Mater. Lett. 62 (2008) 3607–3609. doi:10.1016/j.matlet.2008.04.008.

[10] E. Dogru, A. Demirbas, B. Altinsoy, F. Duman, I. Ocsoy, Formation of Matricaria

chamomilla extract-incorporated Ag nanoparticles and size-dependent enhanced antimicrobial property, J. Photochem. Photobiol. B Biol. 174 (2017) 78–83. doi:10.1016/j.jphotobiol.2017.07.024.

[11] C. Lee, J.Y. Kim, W. I. Lee, K.L. Nelson, J. Yoon, D.L. Sedlak, Bactericidal Effect of Zero-Valent Iron Nanoparticles on Escherichia coli, Environ. Sci. Technol. 42 (2008) 4927–4933. doi:10.1021/es800408u.

[12] M. Diao, M. Yao, Use of zero-valent iron nanoparticles in inactivating microbes, Water Res. 43 (2009) 5243–5251. doi:10.1016/j.watres.2009.08.051.

[13] Y. Cui, Y. Zhao, Y. Tian, W. Zhang, X. Lü, X. Jiang, The molecular mechanism of action of bactericidal gold nanoparticles on Escherichia coli, Biomaterials. 33 (2012) 2327–2333. doi:10.1016/j.biomaterials.2011.11.057.

[14] F.U. Khan, Y. Chen, N.U. Khan, A. Ahmad, K. Tahir, Z.U. Khan, A.U. Khan, S.U. Khan, M. Raza, P. Wan, Visible light inactivation of E. coli , Cytotoxicity and ROS determination of biochemically capped gold nanoparticles, Microb. Pathog. 107 (2017) 419–424. doi:10.1016/j.micpath.2017.04.024.

[15] Q. Ali, W. Ahmed, S. Lal, T. Sen, Novel Multifunctional Carbon Nanotube Containing Silver and Iron Oxide Nanoparticles for Antimicrobial Applications in Water Treatment, Mater. Today Proc. 4 (2017) 57–64. doi:10.1016/j.matpr.2017.01.193.

[16] M. Auffan, W. Achouak, J. Rose, M. Roncato, C. Chanéac, D.T. Waite, A. Masion, J.C. Woicik, M.R. Wiesner, J. Bottero, Relation between the Redox State of Iron-Based Nanoparticles and Their Cytotoxicity toward Escherichia coli, Environ. Sci. Technol. 42 (2008) 6730–6735. doi:10.1021/es800086f.

[17] H. Sadegh, G.A.M. Ali, V.K. Gupta, A.S.H. Makhlouf, R. Shahryari-ghoshekandi, M.N.

Nadagouda, M. Sillanpaa, E. Megiel, The role of nanomaterails as effective adsorbents and their applications in wasterwater treatment, J. Nanostruct. Chem. 7 (2017) 1-14.

[18] E. Megiel, Surface modification usgin TEMPO and its derivatives, Adv. Colloid Interface Sci. 250 (2017) 158-184.

[19] P. Li, J. Li, C. Wu, Q. Wu, J. Li, Synergistic antibacterial effects of β-lactam antibiotic combined with silver nanoparticles, Nanotechnology. 16 (2005) 1912–1917. doi:10.1088/0957-4484/16/9/082.

[20] N. Tran, M. Hocquet, B. Eon, P. Sangwan, J. Ratcliffe, T.M. Hinton, J. White, B. Ozcelik, N.P. Reynolds, B.W. Muir, Non-lamellar lyotropic liquid crystalline nanoparticles enhance the antibacterial effects of rifampicin against Staphylococcus aureus, J. Colloid Interface Sci. 519 (2018) 107–118. doi:10.1016/j.jcis.2018.02.048.

[21] M. Banoee, S. Seif, Z.E. Nazari, P. Jafari-Fesharaki, H.R. Shahverdi, A. Moballegh, K.M. Moghaddam, A.R. Shahverdi, ZnO nanoparticles enhanced antibacterial activity of ciprofloxacin against Staphylococcus aureus and Escherichia coli, J. Biomed. Mater. Res. Part B Appl. Biomater. 93B (2010) 557–561. doi:10.1002/jbm.b.31615.

[22] A. Panáček, L. Kvítek, M. Smékalová, R. Večeřová, M. Kolář, M. Röderová, F. Dyčka, M. Šebela, R. Prucek, O. Tomanec, R. Zbořil, Bacterial resistance to silver nanoparticles and how to overcome it, Nat. Nanotechnol. 13 (2018) 65–71. doi:10.1038/s41565-017-0013-y.

[23] D. Lantagne, J. Rayner, A. Mittelman, K. Pennell, Comment on "A re-assessment of the safety of silver in household water treatment: rapid systematic review of mammalian in vivo genotoxicity studies," Environ. Heal. 16 (2017) 121. doi:10.1186/s12940-017-0334-1.

[24] U.A. Reddy, P.V. Prabhakar, M. Mahboob, Biomarkers of oxidative stress for in vivo assessment of toxicological effects of iron oxide nanoparticles, Saudi J. Biol. Sci. 24 (2017) 1172–1180. doi:10.1016/j.sjbs.2015.09.029.

[25] L. Wang, Z. Dang, Carbon nanotube composites with high dielectric constant at low percolation threshold, Appl. Phys. Lett. 87 (2005) 42903. doi:10.1063/1.1996842.

[26] J. Li, P.C. Ma, W.S. Chow, C.K. To, B.Z. Tang, J. Kim, Correlations between Percolation Threshold, Dispersion State, and Aspect Ratio of Carbon Nanotubes, Adv. Funct. Mater. 17 (2007) 3207–3215. doi:10.1002/adfm.200700065.

[27] F.H. Gojny, M.H.G. Wichmann, B. Fiedler, I.A. Kinloch, W. Bauhofer, A.H. Windle, K. Schulte, Evaluation and identification of electrical and thermal conduction mechanisms in carbon nanotube/epoxy composites, Polymer (Guildf). 47 (2006) 2036–2045. doi:10.1016/j.polymer.2006.01.029.

[28] K. Sanada, Y. Tada, Y. Shindo, Thermal conductivity of polymer composites with close-packed structure of nano and micro fillers, Compos. Part A Appl. Sci. Manuf. 40 (2009) 724–730. doi:10.1016/j.compositesa.2009.02.024.

[29] J. Kimling, M. Maier, B. Okenve, V. Kotaidis, H. Ballot, A. Plech, Turkevich Method for Gold Nanoparticle Synthesis Revisited, J. Phys. Chem. B. 110 (2006) 15700–15707. doi:10.1021/jp061667w.

[30] V. Maheshwari, J. Kane, R.F. Saraf, Self-assembly of a Micrometers-long One-dimensional network of cemented Au nanoparticles, Adv. Mater. 20 (2008) 284–287.

[31] H. Zhang, D. Wang, Controlling the growth of Charged-nanoparticle chains through interparticle electrostatic repulsion, Angew. Chem. Int. Ed. 47 (2008) 3984-3987.

[32] K. Yoosaf, B.I. Ipe, C.H. Suresh, K.G. Thomas, In situ synthesis of metal nanoparticles

and selective Naked-eye detection of lead ions from aqueous media, J. Phys. Chem. C 111 (2007) 12839-12847.

[33] M. Hong, L. Wu, L. Tian, J. Zhu, Controlled assembly of Au, Ag, and Pt nanoparticles with chitosan, Chem. Eur. J. 15 (2009) 5935-5941.

[34] C. Hu, K. Lin, X. Wang, S. Liu, J. Yi, Y. Tian, B. Wu, G. Chen, H. Yang, Y. Dai, H. Li, N. Zheng, Electrostatic Self-assembling formation of Pd superlattice nanowire from Surfactant-free ultrathin Pd nanosheets, J. Am. Chem. Soc. 136 (2014) 12856-12859.

[35] J. Drbohlavova, R. Hrdy, V. Adam, R. Kizek, O. Schneeweiss, J. Hubalek, Preparation and properties of various magnetic nanoparticles, Sensors. 9 (2009) 2352–2362. doi:10.3390/s90402352.

[36] S.K. Sahoo, K. Agarwal, A.K. Singh, B.G. Polke, K.C. Raha, Characterization of γ- and α-Fe 2 O 3 nano powders synthesized by emulsion precipitation-calcination route and rheological behaviour of α-Fe_2O_3, Sci. Technol. 2 (2010) 118–126. doi:10.4314/ijest.v2i8.63841.

[37] G. Wang, Y. Ling, D.A. Wheeler, K.E.N. George, K. Horsley, C. Heske, J.Z. Zhang, Y. Li, Facile Synthesis of Highly Photoactive α-Fe_2O_3 -Based Films for Water Oxidation, Nano Lett. 11 (2011) 3503–3509. doi:10.1021/nl202316j.

[38] T. Fujii, F.M.F. de Groot, G.A. Sawatzky, F.C. Voogt, T. Hibma, K. Okada, In situ XPS analysis of various iron oxide films grown by NO_2 -assisted molecular-beam epitaxy, Phys. Rev. B. 59 (1999) 3195–3202. doi:10.1103/PhysRevB.59.3195.

[39] E. McCafferty, J.P. Wightman, Determination of the concentration of surface hydroxyl groups on metal oxide films by a quantitative XPS method, Surf. Interface Anal. 26 (1998) 549–564. doi:10.1002/(SICI)1096-9918(199807)26:8<549::AID-

SIA396>3.3.CO;2-H.

[40] X. Lu, G. Wang, T. Zhai, M. Yu, J. Gan, Y. Tong, Y. Li, Hydrogenated TiO 2 Nanotube Arrays for Supercapacitors, Nano Lett. 12 (2012) 1690–1696. doi:10.1021/nl300173j.

[41] N.R. Jana, L. Gearheart, C.J. Murphy, Wet chemical synthesis of high aspect ratio cylindrical gold nanorods, J. Phys. Chem. B. 105 (2001) 4065–4067. doi:10.1021/jp0107964.

[42] L. Pu, M. Baig, V. Maheshwari, Nanoparticle chains as electrochemical sensors and electrodes, Anal. Bioanal. Chem. 408 (2016) 2697–2705. doi:10.1007/s00216-015-9287-9.

[43] J. Luo, S. Jiang, H. Zhang, J. Jiang, X. Liu, A novel non-enzymatic glucose sensor based on Cu nanoparticle modified graphene sheets electrode, Anal. Chim. Acta. 709 (2012) 47–53. doi:10.1016/j.aca.2011.10.025.

[44] Y. Wang, X. Teng, J. Wang, H. Yang, Solvent-Free Atom Transfer Radical Polymerization in the Synthesis of Fe_2O_3@Polystyrene Core−Shell Nanoparticles, Nano Lett. 3 (2003) 789–793. doi:10.1021/nl034211o.

[45] J. Tam, S. Salgado, M. Miltenburg, V. Maheshwari, Electrochemical synthesis on single cells as templates, Chem. Commun. 49 (2013) 8641. doi:10.1039/c3cc44308f.

[46] P. Krystosiak, W. Tomaszewski, E. Megiel, High-density polystyrene-grafted silver nanoparticles and their use in the preparation of nanocomposites with antibacterial properties, J. Colloid Interface Sci. 498 (2017) 9-21.

[47] Z. Dang, K. Shehzad, J. Zha, A. Mujahid, T. Hussain, J. Nie, C. Shi, Complementary percolation characteristics of carbon fillers based electrically percolative thermoplastic elastomer composites, Compos. Sci. Technol. 72 (2011) 28–35.

doi:10.1016/j.compscitech.2011.08.020.

[48] Q. Lin, S. Mahendra, D.Y. Lyon, L. Brunet, M.V. Liga, D. Li, P.J.J. Alvarez, Antimicrobial nanomaterails for water disinfection and microbial control: Potential applications and implication, Water Res. 42 (2008) 4591-4602.

[49] A Wave of Resurgent epidemics has hit the U.S., Sci. Amer. 318 (2018) 44-57.

[50] X. Wu, Y. Lu, S. Zhou, L. Chen, B. Xu, Impact of climate change on human infectious diseases: Emprical evidence and human adaptation, Environ. Int. 86 (2016) 14-23.

[51] I. delpla, A-V. Jung, E. Baures, M. Clement, O. Thomas, Impacts of climate change on surface water qualtiy in relation to drinking water production, Environ. Int. 35 (2009) 1225-1233.

Graphical abstract

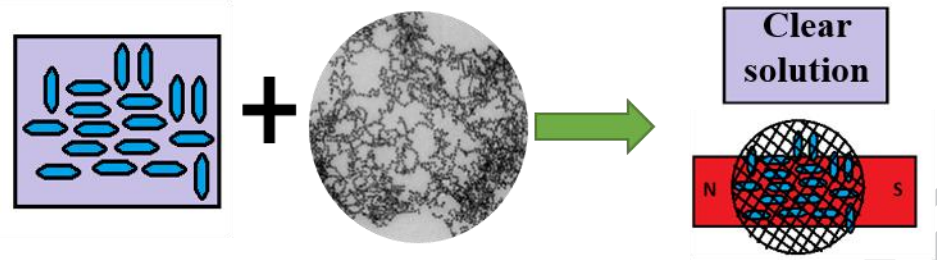

Magnetic nano-nets capture the cells and are removed by a magnet